jove

Contribution of the Na$^+$/K$^+$ Pump to Rhythmic Bursting, Explored with Modeling and Dynamic Clamp Analyses

Ricardo Javier Erazo-Toscano[1,2], **Parker J. Ellingson**[2], **Ronald L. Calabrese**[1], **Gennady S. Cymbalyuk**[2]

[1] Department of Biology, Emory University [2] Neuroscience Institute, Georgia State University

[*] These authors contributed equally

Corresponding Author

Ronald L. Calabrese
biolrc@emory.edu

Abstract

The Na$^+$/K$^+$ pump, often thought of as a background function in neuronal activity, contributes an outward current (I_{pump}) that responds to the internal concentration of Na$^+$ ([Na$^+$]$_i$). In bursting neurons, such as those found in central pattern generator (CPG) neuronal networks that produce rhythmic movements, the [Na$^+$]$_i$ and therefore the I_{pump}, can be expected to vary throughout the burst cycle. This responsiveness to electrical activity, combined with independence from membrane potential, endow I_{pump} with dynamical properties not common to channel-based currents (e.g., voltage- or transmitter-gated or leak channels). Moreover, in many neurons, the pump's activity is modulated by a variety of modulators, further expanding the potential role of I_{pump} in rhythmic bursting activity. This paper shows how to use a combination of modeling and dynamic clamp methods to determine how I_{pump} and its interaction with persistent Na$^+$ current influence rhythmic activity in a CPG. Specifically, this paper will focus on a dynamic clamp protocol and computational modeling methods in heart interneurons of medicinal leeches.

Introduction

Heartbeat in leeches is driven by a CPG consisting of 9 bilateral pairs of heart interneurons (HNs) distributed across as many mid-body segmental ganglia. At the core of the CPG are mutually inhibitory pairs of interneurons located in the 3rd and 4th segmental ganglia that form half-center oscillators (HCOs) (**Figure 1A**). These neurons continue to burst when synaptically isolated pharmacologically using bicuculline[1].

Others, such as the pair in the 7th segmental ganglia (the focus of this protocol), are also bursters, capable of producing bursting activity when synaptically isolated. They are not mutually connected and receive only descending input, and thus are easily isolated by severing the ganglion from the rest of the nerve cord. This independent bursting activity is sensitive to introduced leak current caused by penetration

with sharp microelectrodes for recording but vigorously burst when recorded with loose patch methods[1].

Both individual HN neurons and HN HCOs have been modeled (Hodgkin-Huxley-based single isopotential compartment models of HN neurons containing all experimentally identified voltage-gated and synaptic currents), and all the burst characteristics of the living system have been successfully captured[2]. Myomodulin, an endogenous neuropeptide in leeches, markedly decreases the period (T) of the burst rhythm of isolated HN neurons and HN HCOs. This modulator acts to increase h-current (hyperpolarization-activated inward current, I_h) and to decrease I_{pump}[3]. This observation led to the exploration of how I_{pump} interacts with I_h, and how their co-modulation contributes to the rhythmic activity of HN neurons. Activation of the pump by increasing $[Na^+]_i$ (using the ionophore monensin) speeds the HN burst rhythm in both HN HCOs and isolated HN neurons[4]. This speed-up was dependent on I_h. When I_h was blocked (2 mM Cs^+), the burst period was not altered by this method of pump activation; however, the burst duration (BD) was curtailed, and the interburst interval (IBI) increased in both HN HCOs and isolated HN neurons[4].

For this protocol, all the currents of a living HN(7) neuron, including the pump current, I_{pump}, are incorporated in the HN model as follows:

$$C\frac{dV}{dt} = -\big(I_{Na} + I_P + I_{K1} + I_{K2} + I_{KA} + I_h$$
$$+ I_{CaF} + I_{CaS} + I_{Leak} + I_{pump}\big) \quad (1)$$

where C is the membrane capacitance (in nF), V is the membrane potential (in V), t is time (in s). Detailed ionic current descriptions and equations have been described elsewhere[2,4]. The complete HN model neuron runs in real time (**Figure 2**). The software will be made available on GitHub upon publication and will be suitable to run on the digital signal processing board described in the **Table of Materials**. Here, the focus of enquiry is the Na^+/K^+ pump current (I_{pump}) and the voltage-gated currents contributing significant Na^+ flux: a fast Na^+ current (I_{Na}) and a persistent Na^+ current (I_P). The maximal conductances of these currents are $\bar{g}_{Na}$ and $\bar{g}_P$ respectively. The Na^+/K^+ pump exchanges three intracellular Na^+ ions for two extracellular K^+ ions, thus producing a net outward current. Importantly, it pumps 3 times as much Na^+ out of the neuron as this current indicates, which is important for calculating the intracellular Na^+ concentration.

The Na^+/K^+ pump current depends on intracellular Na^+ concentrations and is expressed by the following sigmoidal function:

$$I_{pump} = \frac{I_{pump}^{max}}{1+\exp\left(\frac{[Na]_{ih}-[Na]_i}{[Na]_{is}}\right)} \quad (2)$$

where $[Na]_i$ is the intracellular Na^+ concentration, I_{pump}^{max} is the maximal Na^+/K^+ pump current, $[Na]_{ih}$ is the intracellular Na^+ concentration for the half-activation of the Na^+/K^+ pump, and $[Na]_{is}$ the sensitivity of the Na^+/K^+ pump to $[Na]_i$. $[Na]_i$ builds as a result of the Na^+ influxes carried by I_P and I_{Na} and is diminished by the Na^+ efflux of the Na^+/K^+ pump. The contribution of I_h and I_{Leak} to the total Na^+ flux is small and is not considered in the real-time model.

$$\frac{d[Na]_i}{dt} = -\frac{I_P + I_{Na} + 3\,I_{pump}}{vF} \quad (3)$$

where, v is the volume (~6.7 pL) of the intracellular Na^+ reservoir, F is Faraday's constant, and the extracellular Na^+ concentration is kept constant.

Voltage-gated and leak conductances have been differentiated-these respond to membrane potential - from the pump current, which is regulated by the calculated intracellular Na$^+$ concentration ([Na$^+$]$_i$). [Na$^+$]$_i$ is built up through Na$^+$ entry via the fast Na$^+$ current (I_{Na}) that produces action potentials (spikes) and the persistent Na$^+$ current (I_P) that provides the depolarization to support spiking. [Na$^+$]$_i$ is, in turn, reduced by the action of the pump through the extrusion of Na$^+$. Baseline living HN values of $\bar{g}_P$(5nS) and $\bar{g}_{Na}$(150 nS) have been assumed, and we take account of any added dynamic clamp $\bar{g}_P$.

The goal of the protocol described here is to manipulate I_{pump} precisely and reversibly in real time to discover how it interacts with voltage-gated currents (persistent Na$^+$ current in the current protocol) to control rhythmic bursting in single HNs. To accomplish this goal, dynamic clamp was used, which artificially introduces, upon command, a precise amount of any current that can be calculated as the model is running. This method has advantages over pharmacological manipulation of the pump, which affects the entire tissue, can have off-target effects that are often hard to reverse, and cannot be precisely manipulated. Dynamic clamp[5,6] reads the voltage of a recorded neuron in real time (**Figure 1B**) and calculates and injects, in real time, the amount of any current based on model equations and the set values of any $\bar{g}_x$ or I_x^{max}. Similar methods can easily be applied to any neuron that can be recorded intracellularly. However, parameters will have to be rescaled to the neuron chosen, and the neuron should be isolated from synaptic inputs, e.g., pharmacologically.

Protocol

NOTE: Invertebrate animal experimental subjects are not regulated by the NIH or Emory and Georgia State Universities. All measures were nevertheless taken to minimize the suffering of the leeches used in this work.

1. Prepare isolated ganglion 7 from the leech nerve cord

1. Maintain leeches *Hirudo verbana* in artificial pond water (containing 0.05% w/v of sea salt) diluted in de-ionized water at 16 °C on a 12:12 light-dark cycle.

2. Prepare the leeches for dissection by cold-anesthetizing them in a bed of crushed ice for >10 min until immobile.

3. Fill a black, resin-lined dissecting dish to a depth of ~1 cm with chilled saline containing 115 mM NaCl, 4 mM KCl, 1.7 mM CaCl$_2$, 10 mM D-glucose, and 10 mM HEPES in de-ionized water; pH adjusted to 7.4 with 1 M NaOH. Pin the leech dorsal side up in the black resin-lined chamber (at least 20 cm x 10 cm with a depth of at least 2 cm above the resin that is at least 2 cm thick).

4. Under a steromicroscope at 20x magnification with oblique light guide illumination, make a longitudinal cut at least 3 cm long with 5 mm spring scissors through the body wall in the rostral 1/3rd portion of the body. Use pins to pull aside the body wall and expose the internal organs.
    NOTE: Any stored blood meal can be removed by suction with a fire-polished Pasteur pipette.

5. Isolate an individual mid-body ganglion 7 (seventh free segmental ganglion caudal to the brain).

    1. Open the sinus in which the nerve cord resides using the 5 mm spring scissors. Be sure to split the sinus

dorsally and ventrally leaving two strips of sinus. Use sharp #5 forceps to help guide the cutting and hold the sinus.

2. Keep the sinus attached to each of the two bilateral nerve roots that emerge from the ganglion (it adheres tightly to each root) to use these strips of sinus for pinning out the ganglion.

3. Remove the ganglion from the body by cutting the rostral and caudal connective nerve bundles that link the ganglia (as far from the 7th ganglion as possible) and the sinus strips, and then cut the roots lateral to where they emerge from the sinus.

6. Pin the ganglion (using old blunted #5 forceps) with shortened minuten insect pins, ventral side up, in clear, resin lined Petri dishes. Insert pins in the strips of sinus and loose tissue adhering to the roots and the rostral and caudal connectives, as far from the ganglion as possible.
NOTE: The resin must be no thicker than 3 mm if good illumination from below is to be achieved during recording. Make sure the ganglion is taut, both longitudinally and laterally

7. Increase the magnification of the stereomicroscope to 40x or greater, and adjust the oblique illumination so the neuronal cell bodies can be easily seen on the ventral surface of the ganglion just below the perineurium.

8. Remove the perineurium of the ganglion (desheath) with microscissors.

   1. Start the desheathing by cutting the loose sheath between the roots on one side, and continue the cut laterally to the other side, making sure to keep the scissor blades superficial and not harm the neuronal cell bodies directly beneath the sheath.

2. Make a similar superficial cut caudally from the lateral cut along the midline.

3. Now grab the caudolateral flap of sheath on one side with the fine #5 forceps, pull it away from the ganglion, and cut it off with the microscissors.

4. Repeat on the other side; this procedure exposes both HN(7) neurons for recording with microelectrodes.

9. Place the preparation dish in the recording setup, and superfuse with saline at a flow rate of 5 mL/min at room temperature.

2. Identify and record leech heart interneurons with sharp microelectrodes

1. For the duration of the recording of the HN(7) neuron (recordings last between 30 to 60 min), acquire and digitize the intracellular current and voltage traces from a neurophysiological electrometer sampling at rate of 5 kHz with a digital data acquisition (Analog to Digital, A to D) and stimulation (Digital to Analog, D to A) system, and display on a computer screen.
NOTE: Any commercial or custom-built software and A to D/D to A board can be used for data acquisition (A to D). D to A and custom-built software are required for dynamic clamp.

2. Under a steromicroscope at 50-100x with dark field illumination from below, tentatively identify an HN(7) neuron of the bilateral pair by its canonical location at the posteriolateral position in midbody ganglion seven.

3. Now aim to penetrate the putative HN(7) neuron with a sharp microelectrode filled with 2 M potassium acetate and 20 mM KCl using a micromanipulator.

1. Place the microelectrode very near the target cell body.

2. Continuously observe the recorded potential with the electrometer, and set this potential to zero mV before penetrating the neuron.

3. Penetrate the neuron with the microelectrode, by slowly driving the electrode along its long axis with the manipulator. Using the electrometer buzz function, set to 100 ms buzz duration, until a negative shift in membrane potential and vigorous spiking activity is observed.

4. Set the electrometer in discontinuous current-clamp mode (DCC) ≥ 3 kHz to simultaneously record membrane potential and pass current with the single microelectrode (capacity compensation set to just below ringing and then dialed back 10%).

   1. Monitor the settling of the electrode during DCC on an oscilloscope.

   2. Inject a steady current of -0.1 nA with the electrometer steady current injector for a minute or two to stabilize the recording.

5. Definitively identify the HN(7) neuron by its characteristic spike shape and weak bursting activity (**Figure 1C*i***).

6. Perform any data analysis offline after the experiment is completed, and save all data on a disk.

3. Build a real-time HN or another model neuron

1. Build custom software using a digital signal processing board (DSB; D to A and A to D) in a desk-top computer to implement in real time the model currents described in[2,4] or different model currents for other neurons or experiments.

   1. Use Hodgkin-Huxley style equations as they are the generally preferred method for representing model currents.

   2. See[7] for a detailed description of the implementation of the real-time HN model and dynamic clamp prior to the addition of the pump current. Refer to the introduction section for the description of the currents, intracellular Na^+ concentration, and conductances of the living HN(7) neuron in the HN model.

4. Implement and vary dynamic clamp conductances/currents

1. Use the custom-built dynamic clamp software for the DSB to implement and change in real time dynamic clamp any of the graphical user interface (**Figure 3**) (GUI)-accessible, programmed conductances and currents of the HN real-time model of the HN(7) neuron.

   NOTE: As a reminder, $\bar{g}_P$ and I_{pump}^{max} are the maximal conductance of the persistent Na^+ current (I_P) and the maximal pump current (I_{pump}), respectively.

2. Use GUI entry boxes in the software to make changes, as the model is running, in the I_{pump}^{max} (PumpMaxL box) and $\bar{g}_P$ (GpinHNLive box) (**Figure 3**).
   NOTE: The GUI input boxes accept typed values, and steps of 0.1 nA are recommended for I_{pump}^{max} and steps of 1 nS are recommended for $\bar{g}_P$.

   1. Add small amounts of I_{pump}^{max} and $\bar{g}_P$ with dynamic clamp to stabilize bursting of the HN(7)

neuron, which is weakened by a microelectrode-induced leak, as shown in **Figure 1Cii**.

NOTE: Sharp microelectrode penetration causes membrane damage that is expressed as increased leak conductance or decreased input resistance.

2. Start by adding a value of $I_{\text{pump}}^{\max}$ of 0.1-0.2 nA, which makes up for the microelectrode-induced leak, but depresses excitability, and then gradually increase $\bar{g}_P$, which increases excitability, until regular bursting ensues, usually at $\bar{g}_P$ of ~1-4 nS (**Figure 4A**).

3. Systematically co-vary these currents (increments of 0.1 nA for $I_{\text{pump}}^{\max}$ and 1 nS for $\bar{g}_P$) to the recorded HN(7) neuron with dynamic clamp (**Figure 3**), and assess their effects on burst characteristics: spike frequency (f: the reciprocal of the average of the interspike interval during a burst), interburst interval (IBI: the time between the last spike in one burst to the first spike in the next burst), burst duration (BD: the time between the first spike in a burst and the last spike in a burst), and burst period (T: the time between the first spike in a burst and the first spike in the subsequent burst).

    1. Change the values of $I_{\text{pump}}^{\max}$ and $\bar{g}_P$, as in the video demonstration, to become familiar with the technique and then venture out.

        1. Hold $I_{\text{pump}}^{\max}$ at a specific fixed value and sweep in 1 nS increments over a range of $\bar{g}_P$ supporting regular bursting activity.

2. Now increase the fixed value of $I_{\text{pump}}^{\max}$ by 0.1 nA and again sweep over a range of $\bar{g}_P$ supporting regular bursting activity.

3. For each implemented parameter pair, collect data containing at least 8 bursts so that reliable average measures of f, IBI, BD, and T can be made.

4. Continue with sweeps for as long as the neuron remains viable, as assessed by strong spiking and a stable baseline potential of oscillation.

5. Collect data from several neurons (from different animals) to generate a composite graph (**Figure 5**).

Representative Results

Modeling with the addition of I_{pump}[4] brought the experimental findings presented in the introduction section into sharper focus and began to explain the pump-assisted mechanism of bursting. The real-time model demonstrated here has been tuned ($\bar{g}_x$ and I_x^{max} parameters chosen) so that it produces regular rhythmic activity falling within the bounds of normal activity as observed in experiments - f, IBI, BD, T - and continues to produce such activity when the myomodulin-modulated parameters I_{pump}^{max} (the maximal pump current) and $\bar{g}_h$ (maximal conductance of h-current) are varied or co-varied in the model. The parameter values determined can be used as a benchmark or canonical set for modeling experiments. In these model instances, I_{pump} oscillates throughout the burst cycle as $[Na^+]_i$ around a baseline level. I_{pump} contributes to burst termination during the burst phase, and the hyperpolarization it produces activates I_h during the IBI; notice the maximal level of I_h near burst initiation (**Figure 2**).

Although the real-time HN model has all implemented currents[2,4] available for dynamic clamping, the focus here was on I_{pump}^{max} and $\bar{g}_P$, which are available for changes while the model is running in the dynamic clamp GUI (**Figure 3**). Dynamic clamp allows the experimenter to add (or subtract with a negative $\bar{g}_x$ or I_x^{max}) any conductance or current into a neuron artificially that mimics the voltage and ionic dependence of a real conductance or current. Thus, it is possible to fully explore how a particular conductance/current interacts with the endogenous conductances/currents inside cells (**Figure 1**). The real-time HN model indicates that the persistent Na$^+$ current (I_P) in HN neurons contributes much of the Na$^+$ entry strongly affecting $[Na^+]_i$ (**Figure 2**) and thus, I_{pump}. Because I_P is active at relatively negative membrane potentials, it opposes I_{pump} even during the IBI.

These observations indicate that it is instructive to explore interactions between I_x^{max} and $\bar{g}_P$ in isolated HN neurons with dynamic clamp as discussed previously[8,9,10]. These experiments (ongoing) are performed with sharp microelectrode recordings in single, synaptically isolated HN(7) neurons (seventh ganglion severed from the nerve cord). To date, these experiments show that robust bursting is restored in tonically active HN neurons (due to microelectrode penetration introduced leak) by co-addition of I_P and I_{pump} with dynamic clamp (**Figure 4**). This is an important observation indicating that a bursting mechanism is available in these neurons (even when leak is compromised) that results from the interaction of I_{pump} and I_P. Preliminary results indicate their strong complicated interaction, which can be explored in the model and experiments (**Figure 5**).

In conclusion, I_{pump} in response to periodic increases in $[Na^+]_i$ during bursting activity contributes to the burst rhythm through burst termination (decreasing BD). The interaction of I_P and I_{pump} constitutes a mechanism that is sufficient to support endogenous bursting activity; this mechanism can reinstate robust bursting in HN interneurons recorded intracellularly in ganglion 7. The interaction between I_P and I_{pump} through $[Na^+]_i$ affects the HN burst period non-monotonically and ensures robustness of autonomous bursting. These conclusions are in line with experiments and modeling in vertebrate systems[11,12].
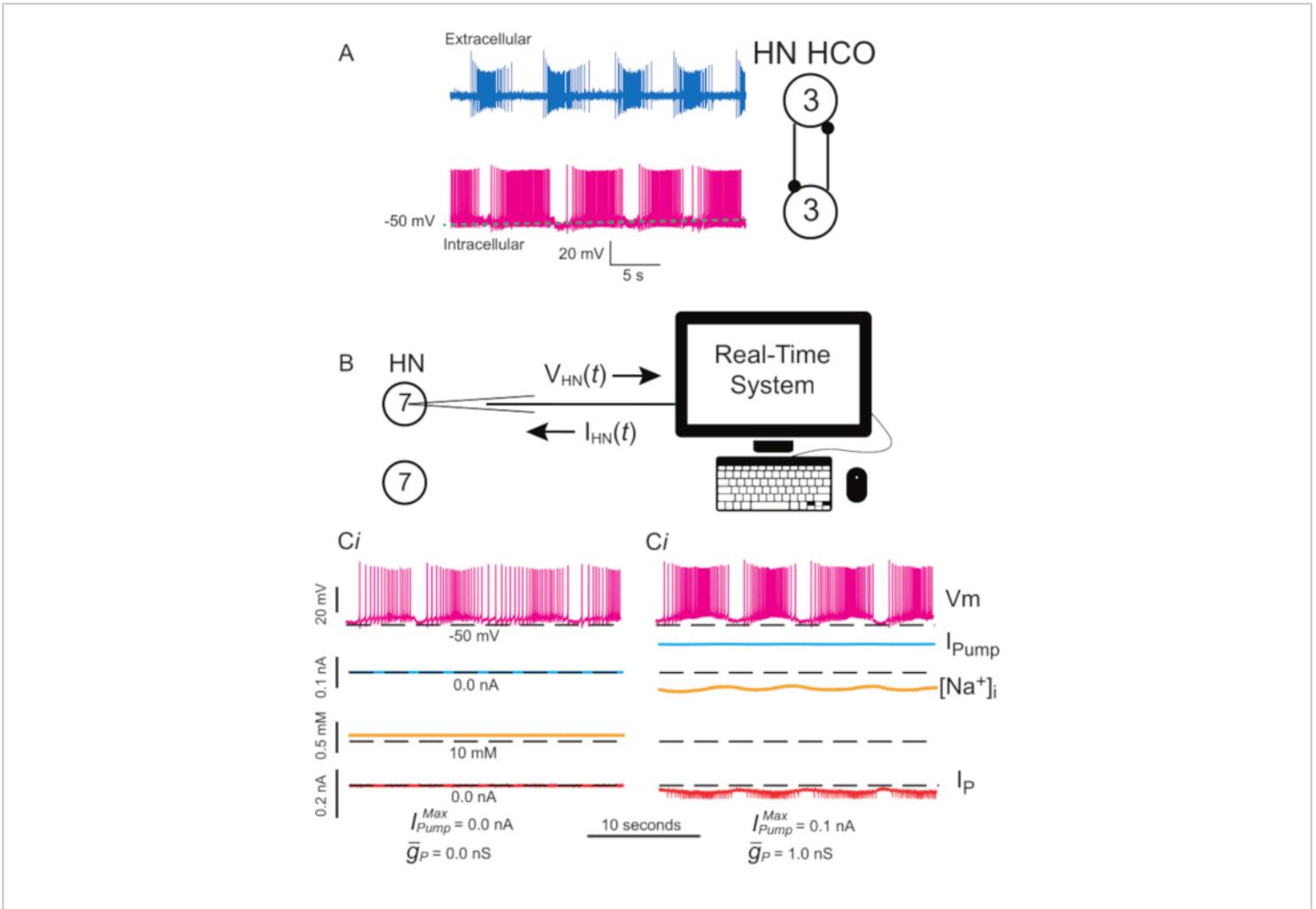
Figure 1: Leech heart interneuron electrical activity and implementation of I_{pump} and I_P with dynamic clamp. (A) Normal bursting activity simultaneously recorded, extracellularly (top) and intracellularly (bottom), in a leech heartbeat HCO from a third ganglion, a schematic of the recorded neurons and their mutually inhibitory synaptic connections at right. **(B)** Dynamic clamp schematic when recording a HN(7) interneuron in an isolated ganglion 7; note there is no synaptic interaction between the two HN(7) interneurons. **(Ci)** Bursting in a leak-compromised HN(7) interneuron. **(Cii)** More robust bursting can be produced by adding dynamic clamp I_{pump} (I_{pump}^{max} = 0.1 nA), which makes up for the microelectrode induced leak, but depresses excitability, and $\bar{g}_P$ (1 nS), which increases excitability. Black dashed lines indicate baseline values. Abbreviations: HN = heart interneuron; HCO = half-center oscillator; I_{pump} = outward current; I_P = persistent Na$^+$ current; I_{pump}^{max} = maximal Na$^+$/K$^+$ pump current; $\bar{g}_P$ = maximal conductance of the persistent Na$^+$ current; Vm = membrane potential; [Na$^+$]$_i$ = internal concentration of Na$^+$. Please click here to view a larger version of this figure.
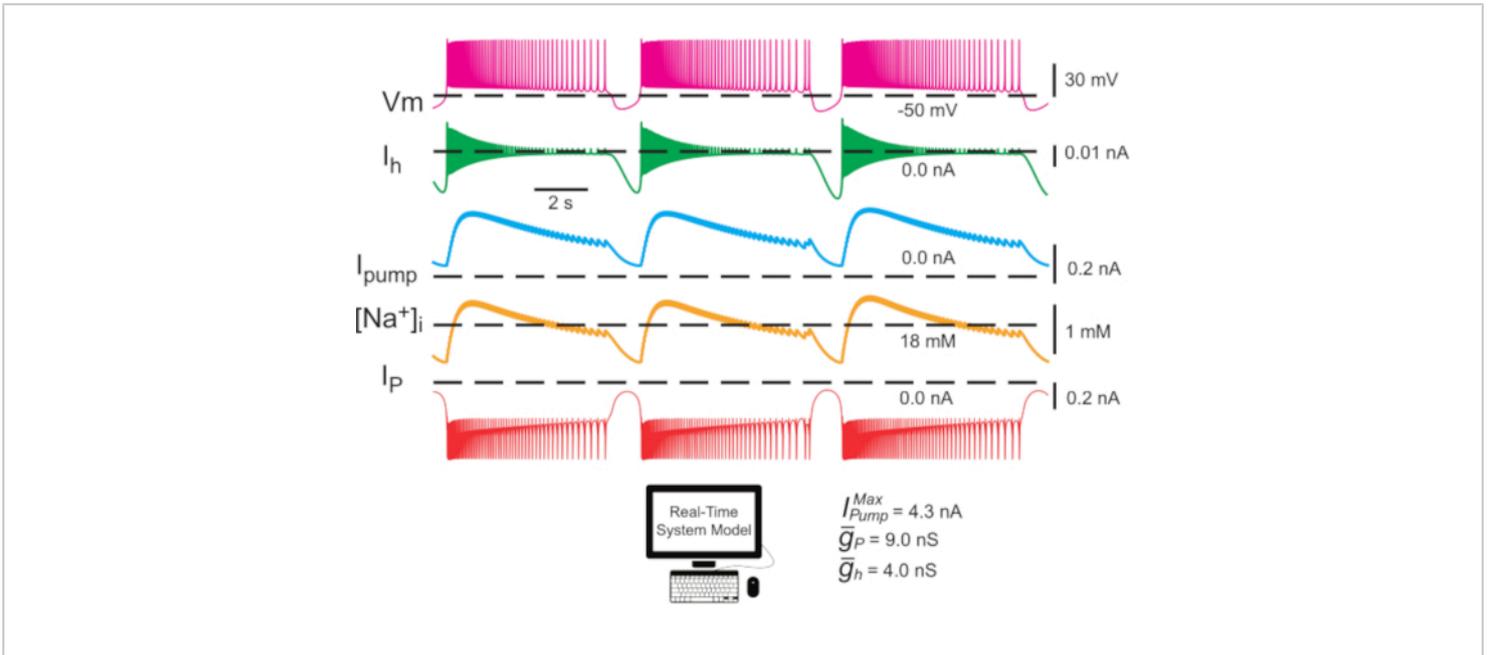
Figure 2: Single HN interneuron model showing traces for membrane potential (Vm), I_h, I_{pump}, $[Na^+]_i$, and I_P. Outward hyperpolarizing currents are negative, and inward depolarizing currents are positive. Black dashed lines indicate baseline values. Abbreviations: HN = heart interneuron; I_{pump} = outward current; I_P = persistent Na^+ current; I_{pump}^{max} = maximal Na^+/K^+ pump current; I_h = hyperpolarization-activated inward current; $\bar{g}_P$ = maximal conductance of the persistent Na^+ current; $\bar{g}_h$ = maximal conductance of the hyperpolarization-activated inward current; Vm = membrane potential; $[Na^+]_i$ = internal concentration of Na^+. Please click here to view a larger version of this figure.
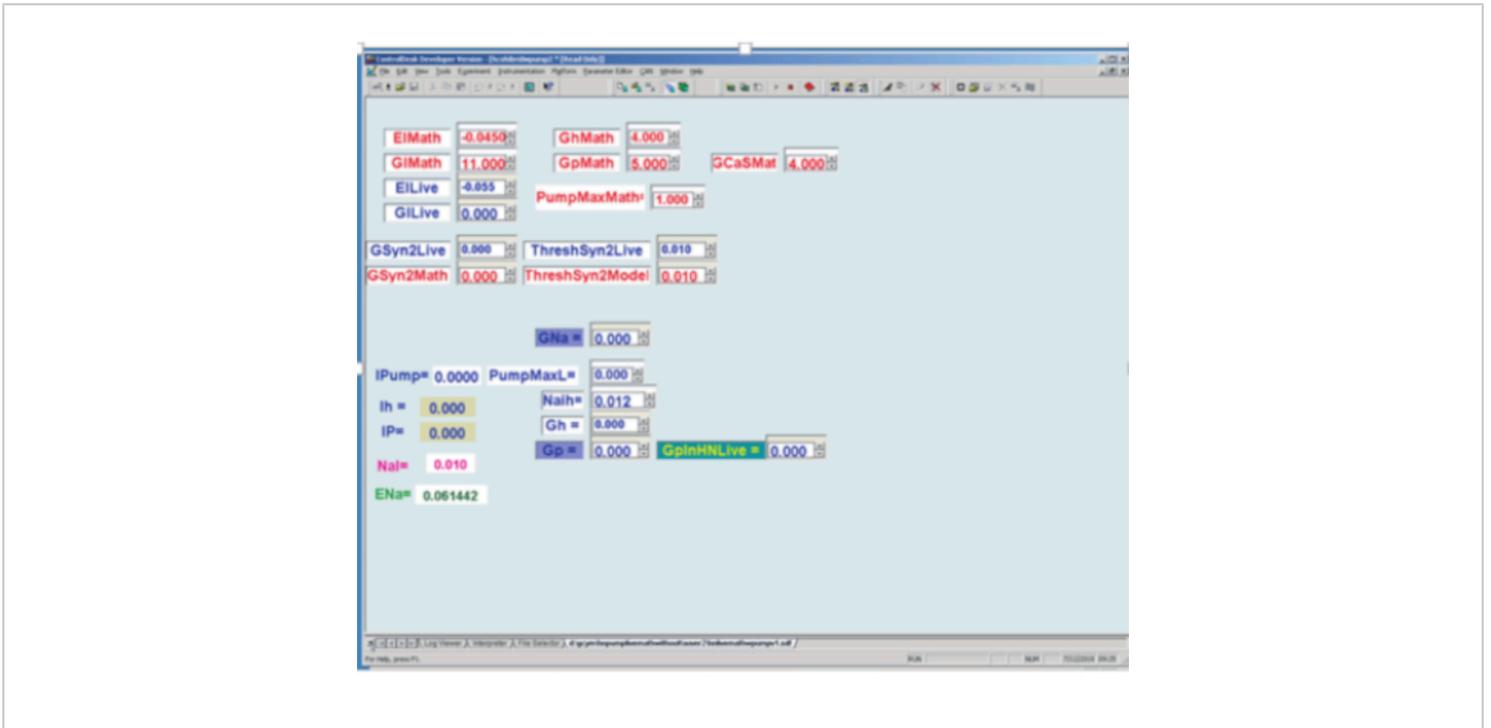
Figure 3: Graphical user interface of real-time heart interneuron (HN) model and dynamic clamp implemented on a digital signal processing board. Upper Left: Red Math boxes are user-determined parameter boxes for the real-time model, whereas Blue Live boxes are user-determined parameter boxes used in the dynamic clamp. El = the reversal potential of the leak current; Gl = leak conductance; Gh = h-current maximal conductance; Gp = P current maximal conductance; GCaS = slow calcium current maximal conductance; PumpMax = pump maximal current; [GSyn2 maximal synaptic conductance to the respective neuron; ThreshSyn2 spike crossing threshold for mediating a synaptic potential - these used to make a hybrid (living/model) half-center oscillator not illustrated here.]. Lower Left for Dynamic Clamp. At the very left are 5 computed values of dynamic clamp variables: I_{pump} = pump current injected; Ih = h-current injected (not used here); IP = P current injected; NaI = calculated internal Na^+ concentration; ENa = calculated sodium reversal potential. Lower Left for Dynamic Clamp. To the right of the computed variables are 6 user determined parameter boxes: GNa = assumed endogenous fast sodium maximal conductance use to calculate Na^+ flux associated with action potentials; PumpMaxL = maximal pump current to be injected by dynamic clamp; Naih see equation (2); Gh = maximal conductance to determine h-current to be injected by dynamic clamp; Gp = assumed endogenous P current maximal conductance use to calculate Na^+ flux associated with endogenous P current; GpinHNLive = maximal conductance to determine P current to be injected by dynamic clamp. Please click here to view a larger version of this figure.
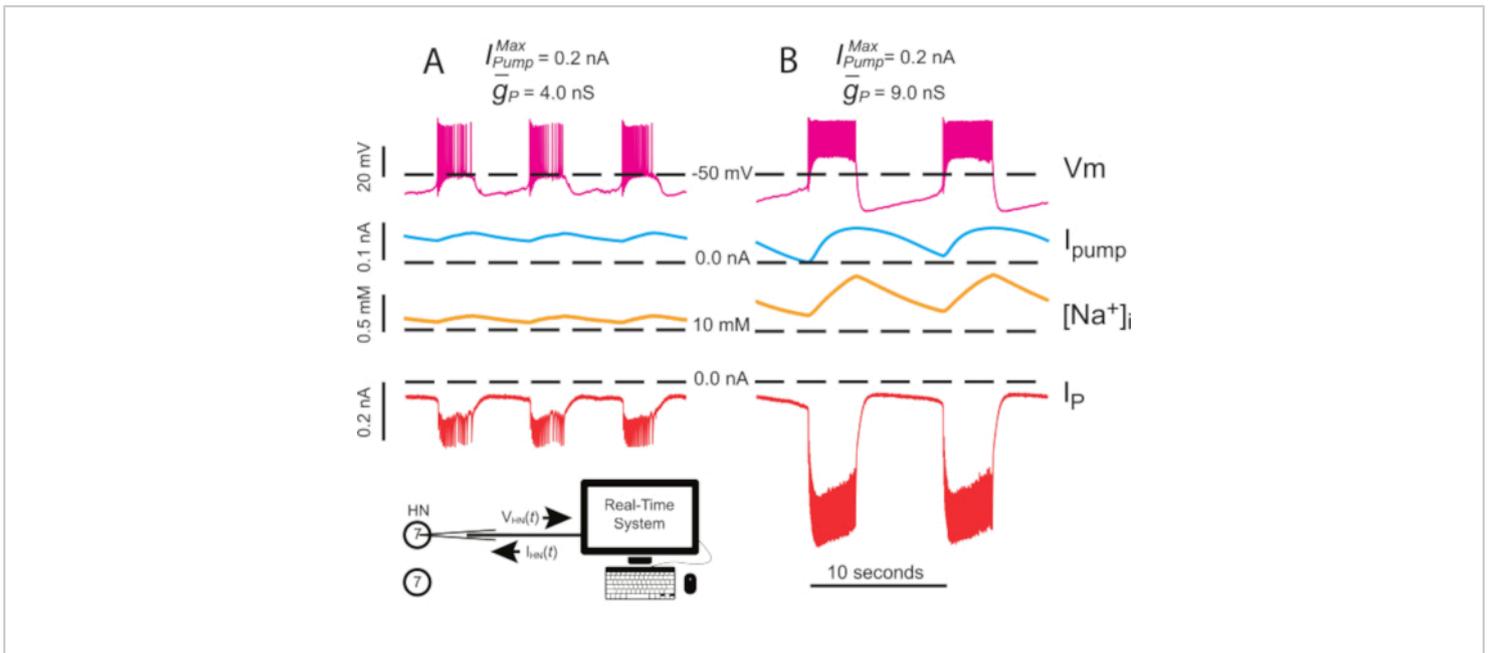
Figure 4: Dynamic clamp analysis of independent HN(7) bursting. Upregulation of $\bar{g}_P$ from (**A**) 4.0 nS to (**B**) 9.0 nS slows down the independent HN burst rhythm. Experimental traces show rhythmic bursting in isolated HN(7) neuron with dynamic clamp. The ranges of oscillation of $[Na^+]_i$ and Vm increase with upregulated $\bar{g}_P$. Traces top to bottom: recorded Vm, injected I_{pump}, calculated $[Na^+]_i$, and injected I_P. Black dashed lines indicate baseline values. Abbreviations: HN = heart interneuron; I_{pump} = outward current; I_P = persistent Na^+ current; I_{pump}^{max} = maximal Na^+/K^+ pump current; $\bar{g}_P$ = maximal conductance of the persistent Na^+ current; Vm = membrane potential; $[Na^+]_i$ = internal concentration of Na^+. Please click here to view a larger version of this figure.
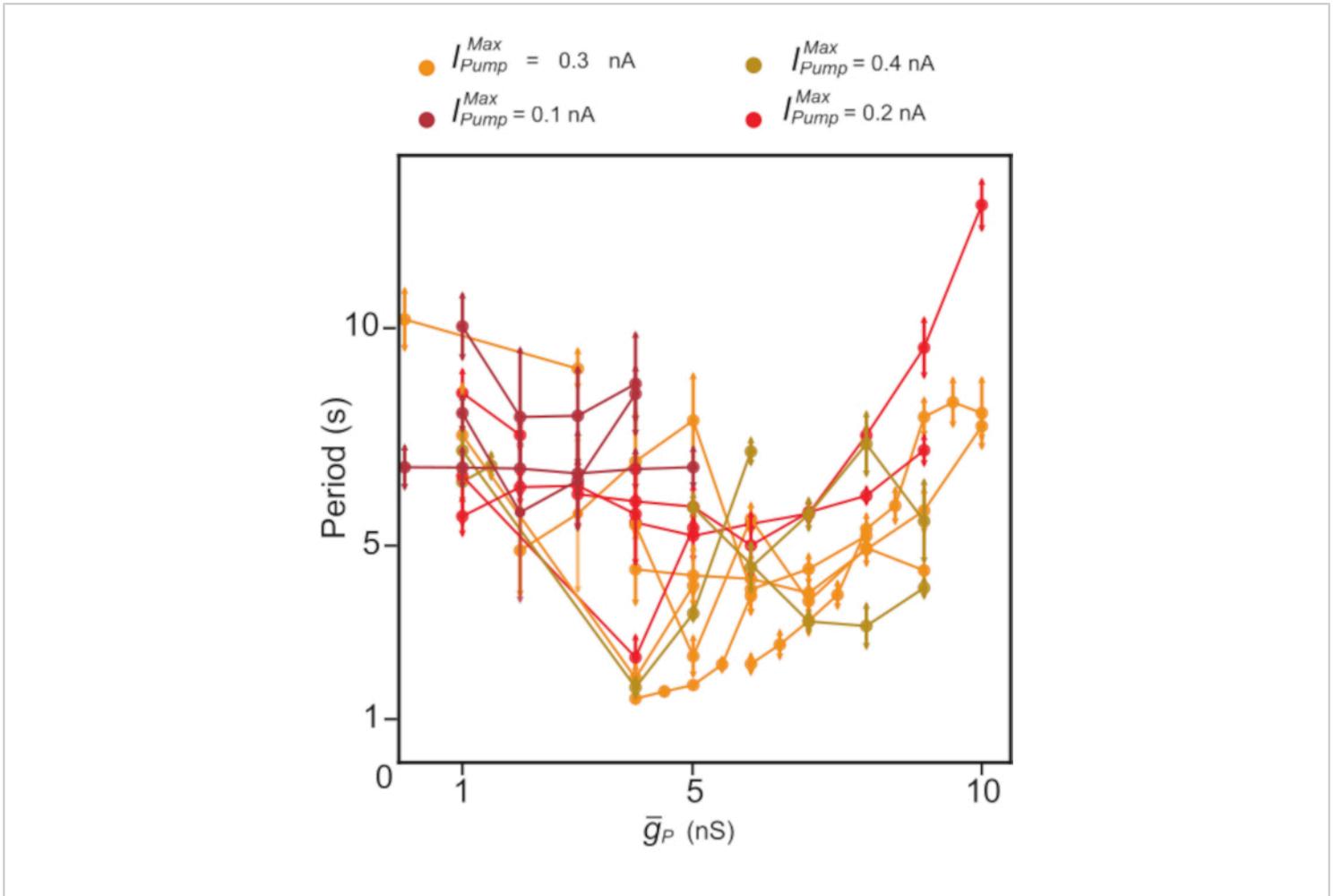
Figure 5: Dynamic clamp analysis of independent HN(7) bursting. Upregulation of $\bar{g}_P$ tends to decrease, followed by an increased HN burst period. In individual experiments (points connected by lines) using dynamic clamp, $\bar{g}_P$ values were swept while I_{pump}^{max} was held constant. Colors represent different constant levels of added I_{pump}^{max} used in different experiments. Abbreviations: HN = heart interneuron; I_{pump}^{max} = maximal Na$^+$/K$^+$ pump current; $\bar{g}_P$ = maximal conductance of the persistent Na$^+$ current. Please click here to view a larger version of this figure.

Discussion

Modeling, dynamic clamp, and the resulting analyses that they enable are useful techniques for exploring how individual and groups of ionic conductance/currents contribute to the electrical activity of neurons (**Figure 1**, **Figure 2**,**Figure 4**, and **Figure 5**). The use of these techniques shows how the Na$^+$/K$^+$ pump current (I_{pump}) interacts with voltage-gated currents, particularly the persistent Na$^+$ current (I_P), to promote robust bursting in the leech heartbeat pattern generator's core HNs. By combining dynamic clamp experiments and modeling, it is possible to test models more directly than is possible with ordinary voltage recording

and current clamp techniques. The results gathered from the dynamic clamp experiments (**Figure 5**) will be used to further refine the HN model. The basic method of dynamic clamping demonstrated here can be customized to reflect the properties of any neuron under study if a mathematical model of neuronal currents can be determined with voltage clamp experiments.

Successful completion of the experiments of the type shown here requires careful impalement of an HN or other neuron when using a sharp microelectrode, because strong bursting is curtailed by electrode penetration[1]. (Whole-cell patch recording techniques, which minimize introduced leak, are also applicable to other neurons, but do not work well on leech neurons.) It is critical that the impalement of the HN neuron causes minimal damage to the neuron (added leak), and input resistance should be monitored and must be in the range of 60-100 MOhms for successful experiments[4].

Dynamic clamp is a powerful technique, but it has limitations imposed by neuronal geometry because the artificial conductances are implemented at the site of the recording electrode-usually the cell body-not at the site where rhythm-generating currents are usually localized[5,6,10]. In leech HN neurons, the cell body is electrically close to the integration zone (main neurite) of the neuron where most active currents are localized, and spikes are initiated.

Disclosures

None

Acknowledgments

References

1. Cymbalyuk, G. S., Gaudry, Q., Masino, M.A., Calabrese, R. L. Bursting in leech heart interneurons: cell-autonomous and network-based mechanisms. *Journal of Neuroscience.* **22**, 10580-10592 (2002).

2. Hill, A. A., Lu, J., Masino, M. A., Olsen, O. H., Calabrese, R. L. A model of a segmental oscillator in the leech heartbeat neuronal network. *Journal of Computational Neuroscience.* **10**, 281-302 (2001).

3. Tobin, A. E., Calabrese, R. L. Myomodulin increases Ih and inhibits the NA/K pump to modulate bursting in leech heart interneurons. *Journal of Neurophysiology.* 94, 3938-3950 (2005).

4. Kueh. D., Barnett, W. H., Cymbalyuk, G. S., Calabrese, R. L. Na(+)/K(+) pump interacts with the h-current to control bursting activity in central pattern generator neurons of leeches. *eLife.* **5**, pii: e19322. (2016).

5. Sharp, A. A., O'Neil, M. B., Abbott, L. F., Marder, E. Dynamic clamp: computer-generated conductances in real neurons. *Journal of Neurophysiology.* **69**, 992-995 (1993).

6. Prinz, A. A., Abbott, L. F., Marder, E. The dynamic clamp comes of age. *Trends in Neuroscience.* **27**, 218-224 (2004).

7. Barnett, W., Cymbalyuk, G. Hybrid systems analysis: real-time systems for design and prototyping of neural interfaces and prostheses. In: *Biohybrid systems:*

nerves, interfaces, and machines., 115-138. R. Jung, ed., Wiley VCH Verlag, Weinheim (2011).

8. Sorensen, M., DeWeerth, S., Cymbalyuk, G., Calabrese, R. L. Using a hybrid neural system to reveal regulation of neuronal network activity by an intrinsic current. *Journal of Neuroscience.* **24**, 5427-5438 (2004).

9. Olypher, A., Cymbalyuk, G., Calabrese, R. L. Hybrid systems analysis of the control of burst duration by low-voltage-activated calcium current in leech heart interneurons. *Journal of Neurophysiology.* **96**, 2857-2867 (2006).

10. Calabrese, R. L., Prinz, A. A. Realistic modeling of small neuronal networks. In: *Computational Modeling Methods for Neuroscientists.*, 285-316. E. DeSchutter, ed., MIT Press, MA, USA (2010).

11. Rybak, I. A., Molkov, Y. I., Jasinski, P. E., Shevtsova, N. A., Smith, J.C. Rhythmic bursting in the pre-Bötzinger complex: mechanisms and models. *Progress in Brain Research.* **209**, 1-23 (2014).

12. Picton, L. D., Nascimento, F., Broadhead, M. J., Sillar, K. T., Miles, G. B. Sodium pumps mediate activity-dependent changes in mammalian motor networks. *Journal of Neuroscience.* **37**, 906-921 (2017).